Journal of Organometallic Chemistry 575 (1999) 39–50

Weak interactions and tautomerism in 3,5-dinitrosubstituted 2- and 4-hydroxypyridines and products of their reaction with $[O(AuPPh_3)_3]BF_4$: synthesis, X-ray structure, IR and UV spectroscopy, and quantum chemical calculations

Lyudmila G. Kuz'mina [a,*], Alexander A. Bagatur'yants [b], Judith A.K. Howard [c], Kira I. Grandberg [d], Alexander V. Karchava [d], Elena S. Shubina [e], Liliya N. Saitkulova [e], Ekaterina V. Bakhmutova [e]

[a] *Institute of General and Inorganic Chemistry, Russian Academy of Science, Leninskii pr. 31, Moscow 117907, Russian Federation*
[b] *Center of Photochemistry, Russian Academy of Science, Novator Str. 7a, Moscow 117421, Russian Federation*
[c] *Chemistry Department, Durham University, South Road, Durham DH1 3LE, UK*
[d] *Chemical Department, Moscow State University, Leninskie Gory, Moscow 117234, Russian Federation*
[e] *Institute of Organoelement Compounds, Russian Academy of Science, Vavilov Str. 28, Moscow 117813, Russian Federation*

Received 8 June 1998

Abstract

Products of the interaction of 3,5-dinitrosubstituted *ortho*- and *para*-hydroxypyridines with $[O(AuPPh_3)_3][BF_4]$ are investigated by X-ray crystallography, IR and UV spectroscopy. The structure of the parent organic molecules are investigated by the spectroscopic methods and ab initio quantum chemical calculations. The calculation and spectroscopy show that the corresponding organic molecules can exist in both tautomeric forms. The reaction with the *ortho* isomer results in the N-aurated dimer $\{[NC_5H_2(NO_2)_2O](AuPPh_3)\}_2$ bound through Au···Au interaction. Under similar conditions, the *para* isomer yields a salt of composition $[O(AuPPh_3)_3][NC_5H_2(NO_2)_2O]$. © 1999 Elsevier Science S.A. All rights reserved.

Keywords: Gold(I) compounds; Tautomerism; Weak interaction; X-ray crystallography; IR; UV; Quantum chemical calculations

1. Introduction

This paper contributes to our systematic work in gold(I) chemistry. Here, we have concentrated on gold(I) compounds with potentially tautomeric ligands containing N and O heteroatoms as reaction sites of tautomeric transformations. Compounds of this type are interesting for two reasons. On the one hand, it is well known that monocharged heavy-metal complex cations (HgR^+ or AuL^+, where R is an organic ligand and L is a neutral ligand) behave like a proton in accordance with isolobal analogy. In particular, many prototropic organic compounds have their metallotropic analogs. It is well known that, in prototropic compounds, the active proton is involved in a hydrogen bond between the corresponding heteroatoms. It could be expected that the HgR^+ or AuL^+ moiety in the related metallotropic compounds forms a covalent bond with one of the heteroatoms and a weak secondary bond with another one. A comparative investigation of structural and dynamic properties of these prototropic and metallotropic compounds gives a way of exploring the limits of the analogy between the

---

* Corresponding author. Tel.: +7-095-954-1279; e-mail: kuzmina@ionchran.msk.ru.

PII: S0022-328X(98)00949-8

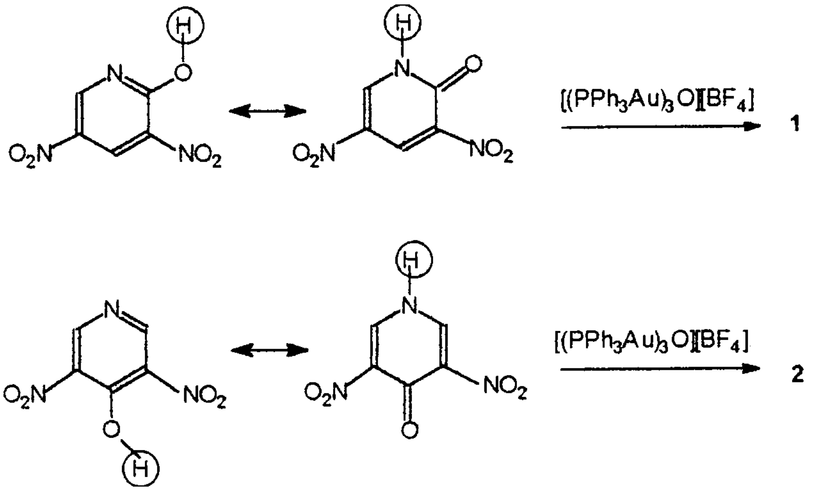

Scheme 1.

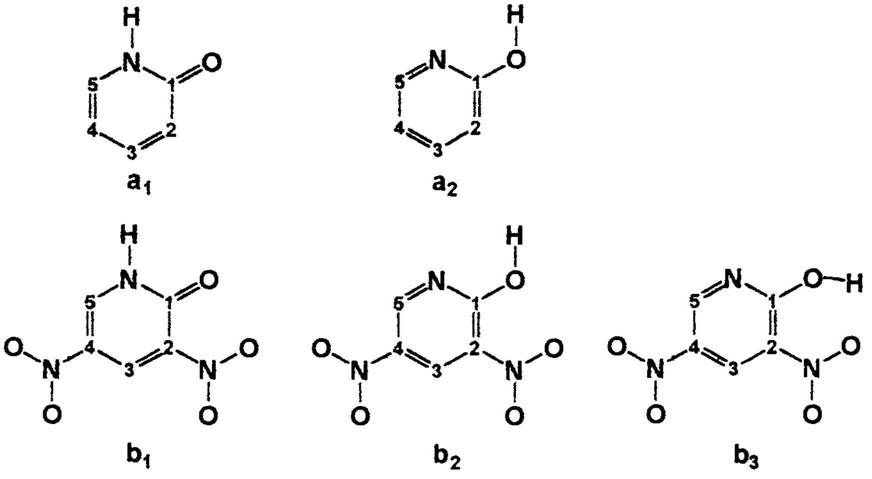

Scheme 2.

corresponding isolobal particles. On the other hand, our preliminary investigations showed that the simple auration of tautomeric organic molecules often results in unpredictable compounds that usually represent small polynuclear gold complexes and that this reaction is accompanied by deep reorganization of the initial organic compounds [1,2]. We suggest that well known gold···gold interactions play a significant role in this process. In order to understand this role in detail we need more structural information about auration products of tautomeric organic molecules.

For these reasons, we launched studies of such compounds. This work is devoted to studying *ortho* and *para* 3,5-dinitrohydroxypyridines and products of their auration with tris(triphenylphosphinegold)oxonium tetrafluoroborate (Scheme 1).

We report here the synthesis of **1** and **2**, IR and UV spectroscopic data for the initial organic compounds and products **1** and **2**, ab initio quantum chemical data for the initial and related organic molecules, and X-ray structures for **1** and **2**.

2. Results and discussion

Instead of the products of simple auration, different and rather unexpected compounds have been obtained in the two above reactions. In the first case (product **1**), a dimer formed via Au···Au interaction was obtained, whereas, in the second case, cation exchange resulted in a salt of $[(AuPPh_3)_3O]^+$ with the corresponding deprotonated organic molecule (product **2**).

2.1. IR and UV spectroscopy of 3,5-dinitro-2-hydroxypyridine and compound 1

The IR spectrum of 3,5-dinitro-2-hydroxypyridine in the solid state shows an intense band at 3220 cm^{-1} typical for a hydrogen-bonded OH group. The bands corresponding to stretching vibrations of the OH and NH groups are lacking in the IR spectrum of **1** in the range 3600–3100 cm^{-1} in the solid state.

The IR spectrum of **1** in the solid state exhibits the following bands in the range of C=O and aromatic C=C

Table 1
Results of quantum chemical calculations of 2-hydroxypyridines (geometrical parameters in Å and °; energy in H)

Molecule	O–C$_1$	N–C$_1$	N–C$_5$	C$_1$–C$_2$	C$_2$–C$_3$	C$_3$–C$_4$	C$_4$–C$_5$	C$_1$NC$_5$	NC$_1$C$_2$	*E*
a$_1$	1.235	1.406	1.366	1.450	1.368	1.423	1.365	126.1	112.6	−322.56927
b$_1$	1.224	1.415	1.462	1.361	1.416	1.365	1.354	126.9	110.8	−730.55488
a$_2$	1.360	1.332	1.349	1.401	1.387	1.399	1.389	117.1	124.4	−322.57289
b$_2$	1.342	1.335	1.407	1.381	1.390	1.389	1.341	119.2	121.6	−730.55551
b$_3$	1.333	1.341	1.333	1.416	1.387	1.382	1.395	119.2	120.7	−730.56002

stretching vibrations: 1644 cm^{-1} attributed to stretching vibrations of the quinoid carbonyl group, ν(C=O) and 1590 cm^{-1} attributed to C=C stretching vibrations of the aromatic heterocycle, ν(C=C).

In CH$_3$CN and THF solutions, ν(C=O) is shifted towards the high-frequency region by about 20 cm^{-1} with respect to the corresponding band observed in the spectrum recorded in nujol, whereas ν(C=C) is almost unchanged.

For the initial organic compound, 3,5-dinitro-2-hydroxypyridine, analogous vibrations in the solid state have the following frequencies: 1700/1690 (doublet), and 1618 cm^{-1}, respectively. In solutions, this band undergoes approximately the same shift as the corresponding band in **1**. Rather intense ν(C=O) (s) and ν(C=C) (m) bands indicate that, in the compound, the pyridine and pyridone structures coexist. The splitting of the ν(C=O) band is, apparently, associated with the formation of a hydrogen-bonded dimer. The high-frequency and low frequency components of the doublet are attributed to vibrations of the free C=O group and the hydrogen-bonded C=O group, respectively [3].

The introduction of the gold-containing group results in a decrease in the ν(C=O) and ν(C=C) frequencies by approximately 55 and 30 cm^{-1}, in accordance with the earlier observation [4]. The vibration bands of nitro groups exhibit a similar shift. The ν_{as}(NO$_2$) band and the main component of the ν_s(NO$_2$) vibration undergo a low-frequency shift by 10–20 cm^{-1} compared to the corresponding bands of 3,5-dinitro-2-hydroxypyridine.The UV spectra of 3,5-dinitro-2-hydroxypyridine in toluene and CH$_3$CN exhibit an intense band at 309–311 nm, with a longwave shoulder at 345–354 nm, which is evidence that the pyridone structure is predominant in these solvents. In THF, the UV spectrum shows an intense and rather sharp band at 334 nm, which indicates that the pyridine structure occurs in this solvent. In toluene and CH$_3$CN, the UV spectrum of **1** shows a band at 340–345 nm with a shoulder at 391–397 nm; which corresponds to a bathochromic shift of 31–34 nm in reference to the initial organic compound. This peculiarity of the UV spectrum is characteristic of an N-aurated coordination compound [5].

Thus, both the IR and UV spectra indicate that compound **1** in the solid state and in solution has the pyridone structure with a covalent Au–N bond. The initial organic compound has the pyridone structure in the solid state, however, it exists in different structures in solution depending on the solvent used.

*2.2. IR and UV spectroscopy of 3,5-dinitro-4-hydroxypyridine and compound **2***

Several intense bands in the range 3700–3000 cm^{-1} attributed to stretching vibrations of the NH and OH groups are observed in the IR spectrum of 3,5-dinitro-4-hydroxypyridine in the solid state.

Intense bands at 1663 and 1685 cm^{-1} are observed in the range 1700–1550 cm^{-1}. These bands are related to ν(C=O) and ν(C=C) vibrations, respectively, which is evidence that the quinoid and benzoid structures of 3,5-dinitro-4-hydroxypyridine coexist in the solid state. A totally different situation is observed in solution. An equilibrium between the pyridone and pyridine forms, apparently, is shifted to the pyridone form because the ν(OH) and ν(C=C) bands almost disappear, and only the ν(NH) and ν(C=O) vibrations remain intense in the spectrum.

As could be expected, no ν(NH) and ν(OH) bands in the range 3600–3100 cm^{-1} are observed in the IR spectrum of **2** in the solid state and in solutions. The IR spectrum of **2** in the solid state in the range 1700–1550 cm^{-1} shows an intense band at 1633 cm^{-1} and a low-intensity band at 1553 cm^{-1}, attributed to ν(C=O) and ν(C=C), respectively. In a THF solution, the ν(C=O) band is shifted toward high frequencies by 8 cm^{-1}; and its intensity retains. At the same time, the ν(C=C) band completely disappears. Thus, the pyridone structure is typical for **2** both in the solid state and in THF solution. The anionic nature of the pyridone moiety in complex **2** is responsible for the reduction of the vibrational frequency of the quinoid carbonyl by 30–40 cm^{-1}.

In the IR spectrum of **2**, the position of ν_{as}(NO$_2$) band (1504 cm^{-1}) remains unchanged, and the ν_s(NO$_2$) bands are shifted toward low frequencies with respect to the initial organic compound (1347 and 1266 cm^{-1}). In **2**, the main band (1266 cm^{-1}) in the range of

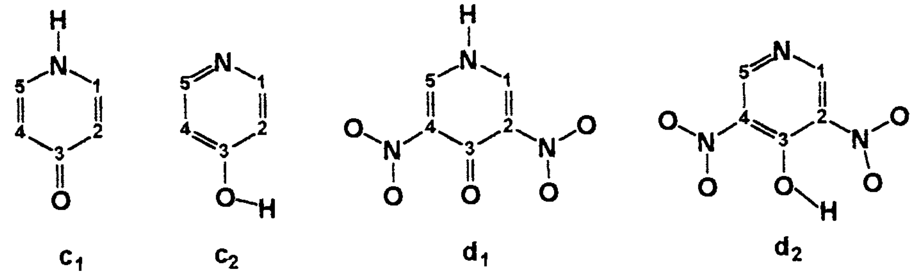

Scheme 3.

nitro-group symmetric vibrations is significantly lower than in **1**, which gives evidence of the ionic nature of the interaction between Au and N.

The UV spectrum of 3,5-dinitro-4-hydroxypyridine in THF (concentration 2×10^{-3} M) displays an intense band at 338 nm typical for the pyridone structure. The electronic spectrum of **2** is significantly different from that of 3,5-dinitro-4-hydroxypyridine.

The UV spectrum of **2** exhibits a doublet at 402–410 nm characteristic of the 3,5-dinitro-4-pyridinolate anion; this doublet is bathochromically shifted by 64–72 nm with respect to the band of the initial neutral compound. Such a significant bathochromic band shift ($\Delta\lambda$) supports the suggestion of the ionic nature of **2**. Note that the absorption of the potassium salt of 3,5-dinitro-4-hydroxypyridine is observed at 393–400 nm with $\Delta\lambda$ equal to 55–62 nm. This hypsochromic shift of the absorption band for the 3,5-dinitro-4-pyridinolate anion in its potassium salt is, probably, associated with the formation of a close ion pair.

Thus, both the IR and UV spectra indicate that compound **2** in the solid state and in solution represents a salt involving 3,5-dinitro-4-pyridinolate as an anion. The quinoid and benzoid structures of 3,5-dinitro-4-hydroxypyridine coexist in the solid state. Predominantly pyridone structure occurs in solutions of this organic compound.

2.3. Quantum chemical calculation of 2- and 4-hydroxypyridines

We carried out ab initio quantum chemical calculations (631G**, MP2) to estimate the relative stability of tautomers of corresponding organic compounds.

Scheme 2 shows the structures of tautomers of 2-hydroxypyridines ($\mathbf{a_1}$ and $\mathbf{a_2}$ are unsubstituted; $\mathbf{b_1}$, $\mathbf{b_2}$, $\mathbf{b_3}$ are 3,5-dinitrosubstituted). Table 1 gives some results of ab initio geometry optimization performed for these structures.

The calculation of two tautomeric forms of unsubstituted 2-hydroxypyridine, $\mathbf{a_1}$ and $\mathbf{a_2}$, resulted in the difference in energies of 2.27 kcal mol^{-1}; form $\mathbf{a_2}$ is slightly more preferable than form $\mathbf{a_1}$. For form $\mathbf{a_2}$, we started our calculation from a non-coplanar orientation of the OH group. It converged to the planar geometry of the molecule, probably, because of the formation of the O–H···N intramolecular hydrogen bond.

In the case of the dinitrosubstituted molecule (**b**), the situation is more complicated. One may suggest two forms for the benzoid tautomer ($\mathbf{b_2}$ and $\mathbf{b_3}$) differing in the orientation of the OH group and, hence, in the mode of the intramolecular hydrogen bond (O–H···N or O–H···O).

In tautomers $\mathbf{b_1}$ and $\mathbf{b_2}$, two nitro groups are differently twisted around the C–N bonds. One of these, at C(4), is almost coplanar with the ring; the corresponding ONCC torsional angle is 0.1° in $\mathbf{b_1}$ and 1.4° in $\mathbf{b_2}$. Another nitro group, at C(2), is twisted by 40.2° in $\mathbf{b_1}$ and by 37.7° in $\mathbf{b_2}$. This rotation is caused by the electrostatic and van der Waals repulsion between two oxygen atoms (of the OH and NO_2 groups). The corresponding O···O distances are equal to 2.834 Å in $\mathbf{b_1}$ and 2.730 Å in $\mathbf{b_2}$. The difference in energy between these two tautomers is negligibly small (0.39 kcal mol^{-1}).

A different situation is observed for benzoid tautomer $\mathbf{b_3}$. This structure is lower in energy than $\mathbf{b_1}$ and $\mathbf{b_2}$ by 3.23 and 2.83 kcal mol^{-1}, respectively. The main distinction between tautomers $\mathbf{b_2}$ and $\mathbf{b_3}$ is the almost coplanar orientation of the nitro group adjacent to OH in $\mathbf{b_3}$ due to intramolecular hydrogen bond OH···O(NO_2) (O···O 2.615 Å, O···H 1.759 Å). This fact gives evidence that the O–H···O(NO_2) hydrogen bond makes a significantly higher contribution in the structure stabilization than any of two possible N–H···O(OH) or O–H···N hydrogen bonds in tautomers $\mathbf{b_1}$ and $\mathbf{b_2}$. Hence, introducing the nitro group in the position adjacent to the OH group of the corresponding organic molecule increases the stabilization of the benzoid structure.

It is of interest to compare the results of our calculations with experimental data. X-ray crystallography shows that substituted 2-hydroxypyridines may exist in both the benzoid and quinoid structures in the solid state. The benzoid structure was observed in 6-bromo-2-hydroxypyridine [6] and 6-chloro-2-hydroxypyridine [7]. The quinoid structure was found for unsubstituted 2-pyridone [8] and in 2-methyl-3,4′-bipyridine-6(1*H*)-one [9]. It was reported that both structural forms of

Table 2
Results of quantum chemical calculations of 4-hydroxypyridines (geometrical parameters in Å and °; energy in H)

Molecule	O–C_3	N–C_1	N–C_5	C_1–C_2	C_2–C_3	C_3–C_4	C_4–C_5	C_1NC_5	$C_2C_3C_4$	*E*
c_1	1.243	1.371	1.371	1.361	1.462	1.462	1.361	120.7	113.5	−322.55230
d_1	1.230	1.363	1.363	1.361	1.475	1.475	1.361	120.9	109.4	−730.53215
c_2	1.366	1.347	1.347	1.391	1.396	1.395	1.394	116.1	118.6	−322.56075
d_2	1.333	1.335	1.345	1.397	1.408	1.405	1.384	116.7	113.9	−730.54816

the hydroxypyridine fragment coexist in the crystal of 2-pyridone-6-chloro-2-hydroxypyridine complex [10]. These experimental results may serve as an illustration for our quantum chemical prediction that the energies of two structural forms is very close to one another. Experimental geometrical parameters for 2-pyridones are very close to our calculated results. For all of the experimental data observed, the following general structural trend is revealed: bonds in the quinoid tautomers alternate and bond lengths in the benzoid tautomers show an aromatic pattern. The calculated bond angles reproduce well the experimental data. The inner bond angle at the nitrogen atom is increased in the quinoid form (126.1°) and reduced in the benzoid form (117.3°). By contrast, the inner angle at the C atom bearing the OH-substituent is reduced in the quinoid form (112.6°) and increased in the benzoid form (124.4°). In addition, it should be noted that the stability of the benzoid form of the heterocyclic system may be increased by introducing a nitro group in the position adjacent to the OH group.

Scheme 3 shows the structures of tautomers of 4-hydroxypyridines (**c_1** and **c_2** are unsubstituted; **d_1** and **d_2**, are 3,5-dinitrosubstituted). Table 2 gives some results of ab initio quantum chemical calculations with the geometry obtained for these structures.

The calculated energies of two tautomeric forms of unsubstituted 4-hydroxypyridine indicate that **c_2** is more stable than **c_1** by 5.30 kcal mol^{-1}. The difference in energy between these tautomers is larger than for 2-hydroxypyridine but is still relatively small, so that the coexistence of both forms cannot be excluded. Both benzoid [11–13] and quinoid [14,15] forms are experimentally observed in substituted 4-hydroxypyridines. The geometrical distortions found in our calculations (the inner angles at N and C(OH) are 116.1 and 118.6° in **c_2** and 120.7 and 113.5° in **c_1**, respectively) are also reproduced in the X-ray experimental data.

The calculation of 3,5-dinitro-4-hydroxypyridine show that form **d_2** is considerably more stable (by 10.0 kcal mol^{-1}) than form **d_1**. This large difference in energy is due to the formation of an intramolecular hydrogen bond between the O–H group and one of the nitro groups. This particular nitro group is almost coplanar with the plane of the heterocycle; the corresponding O–N–C–C torsional angle is 1.9°. At the same time, the corresponding torsional angle for the second nitro group, which does not form a hydrogen bond, is 46.8°. The OH group is coplanar to the heterocycle. In this geometry, the O(nitro)···H bond distance 1.746 Å corresponds to the formation of a hydrogen bond. It should be noted that in **d_1** both nitro groups are twisted from the heterocycle plane around the C–N bond by 39.5°.

In both dinitrosubstituted structures (**b_3** and **d_2**), the supporting effect of the nitro group adjacent to OH is important for the stabilization of the corresponding tautomeric form. By contrast, in the case of the corresponding O-aurated structure, the similar supporting effect is hardly possible. Simple geometrical considerations show that the intramolecular Au···$O(NO_2)$ distance in the corresponding planar six-membered chelate cycle would be even shorter than the typical covalent bond distance, which is sterically prohibited. Hence, the presence of nitro groups does not provide geometrical preferences for the O-aurated structure. On the other hand, the 5-membered chelate cycle (in the case of 2-hydroxypyridines) closed via an Au···O or Au···N secondary bond (an analog of a H-bond in the initial compound) is geometrically favorable. No geometrical restrictions to the formation of the intermolecular Au···O or Au···N secondary bond exist in the case of 4-hydroxypyridines.

Our calculations together with some obvious reasoning show that, in hydroxypyridines, the position of auration depends only on the properties of Au^IL and, probably, may be controlled by introducing various substituents that provide chelate support or affect the charge distribution in the organic ligand.

2.4. X-ray structure of **1**

Structure **1** is shown in Fig. 1 and selected bond lengths and angles are given in Table 3.

The molecule represents a dimer, in which two N-aurated subunits are linked together through the Au···Au aurophilic interaction. The corresponding Au···Au distance 3.1489(8) Å falls within a rather wide range characteristic of such interactions (2.6–3.6 Å [16]). As commonly occurs, two monomeric units are twisted around the Au···Au line. The corresponding torsion angle [P(1)Au(1)Au(2)P(2)] is 109.5°. The Au···Au dis-

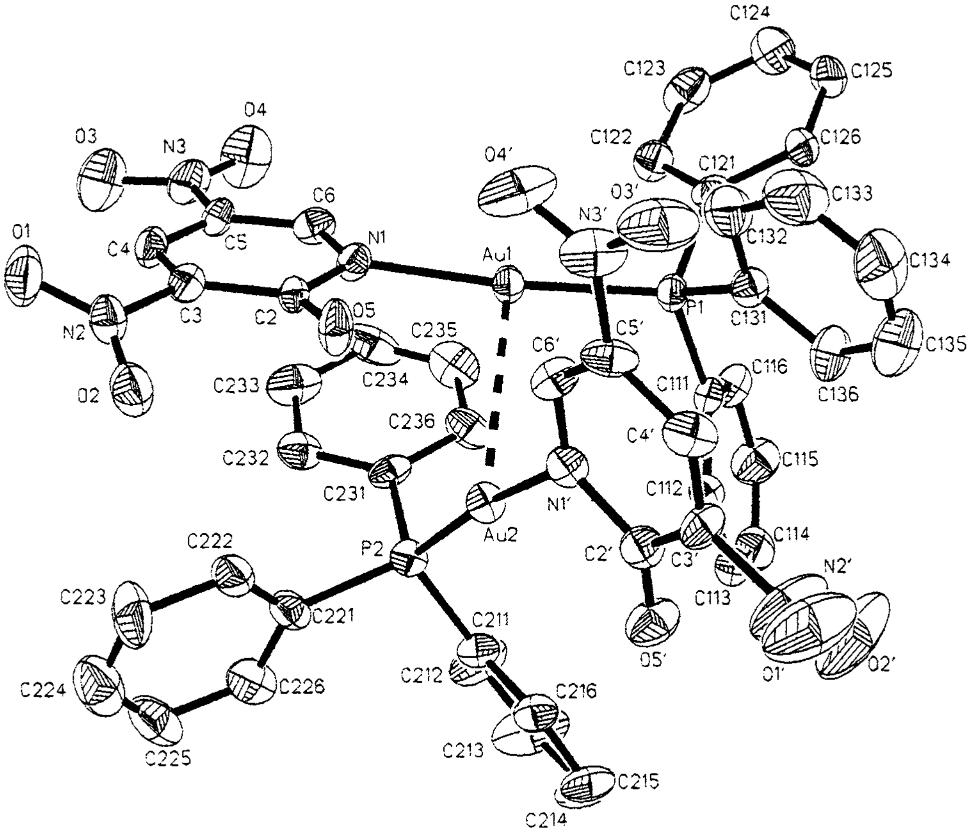

Fig. 1. The molecular structure and numbering scheme for **1**. The hydrogen atoms are omitted.

tances and the torsion angles reported in the literature for other dimeric gold(I)-containing compounds are as follows: in $(C_6H_5SAuPPh_3)_2$, 3.142 Å and 100.8° [16] and 3.155 Å and 100.7° [17]; in $(2\text{-}BrC_6H_4O)AuPPh_3)_2$, 3.245 Å and 112.7° [18].

Table 3
Selected bond lengths (Å) and bond angles (°) for **1**

Au(1)–Au(2)	3.1489(9)	N(1)–C(2)	1.42(1)
Au(1)–N(1)	2.093(8)	N(1′)–C(2′)	1.41(1)
Au(1)–P(1)	2.244(3)	C(2)–C(3)	1.44(1)
Au(2)–N(1′)	2.090(8)	C(2′)–C(3′)	1.47(1)
Au(2)–P(2)	2.237(3)	C(3)–C(4)	1.35(1)
O(5)–C(2)	1.21(1)	C(3′)–C(4′)	1.35(2)
O(5′)–C(2′)	1.19(1)	C(4)–C(5)	1.38(1)
N(1)–C(6)	1.33(1)	C(4′)–C(5′)	1.40(1)
N(1′)–C(6′)	1.32(1)	C(5)–C(6)	1.35(1)
		C(5′)–C(6′)	1.35(1)
N(1)–Au(1)–P(1)	171.3(2)	O(5)–C(2)–C(3)	128.2(9)
N(1′)–Au(2)–P(2)	172.7(2)	O(5′)–C(2′)–C(3′)	126(1)
N(1)–Au(1)–Au(2)	92.1(2)	N(1)–C(2)–C(3)	113.1(8)
N(1′)–Au(2)–Au(1)	91.7(2)	N(1′)–C(2′)–C(3′)	112(1)
C(6)–N(1)–Au(1)	119.6(7)	N(1)–C(6)–C(5)	123(1)
C(6′)–N(1′)–Au(2)	125.9(7)	N(1′)–C(6′)–C(5′)	123.4(9)
C(2)–N(1)–Au(1)	118.7(5)	C(4)–C(3)–C(2)	124.2(9)
C(2′)–N(1′)–Au(2)	111.9(7)	C(4′)–C(3′)–C(2′)	125.3(9)
C(6)–N(1)–C(2)	121.5(8)	C(3)–C(4)–C(5)	118.3(9)
C(6′)–N(1′)–C(2′)	122.2(9)	C(3′)–C(4′)–C(5′)	116.4(9)
O(5)–C(2)–N(1)	118.7(8)	C(6)–C(5)–C(4)	119.4(9)
O(5′)–C(2′)–N(1′)	121.7(9)	C(6′)–C(5′)–C(4′)	120(1)

The similar mutual arrangement of two linear fragments at gold centers in aurophilic dimers was predicted by quantum chemical calculations [19]. It is of interest that the isoelectronic linear mercury compounds RHgX (R = organic ligand and X = heteroatom) never form an analogous twisted structural motif. In vast majority, linear mercury compounds are characterized by antiparallel displaced arrangement of the linear fragment with short contacts between the Hg and X atoms:

$$\begin{array}{ccccc} R- & Hg & - & X & \\ & \vdots & & \vdots & \\ & X & - & Hg & -R \end{array}$$

In the quoted 14-electronic gold complexes [16–18], Au(I) exhibits no tendency to compensate the electron deficit through the formation of an intermolecular secondary bond with a heteratom. The ability of the monocharged gold cation to form gold···gold rather than gold···heteroatom intermolecular secondary bonds is a specific feature of gold(I) compounds.

In each monomeric unit of **1**, gold is attached to nitrogen rather than oxygen. The Au–N (2.093(8) and 2.090(8) Å) and Au–P (2.244(3) and 2.237(3) Å) bond lengths are in correspondence with the commonly observed values in compounds containing the N–Au–P

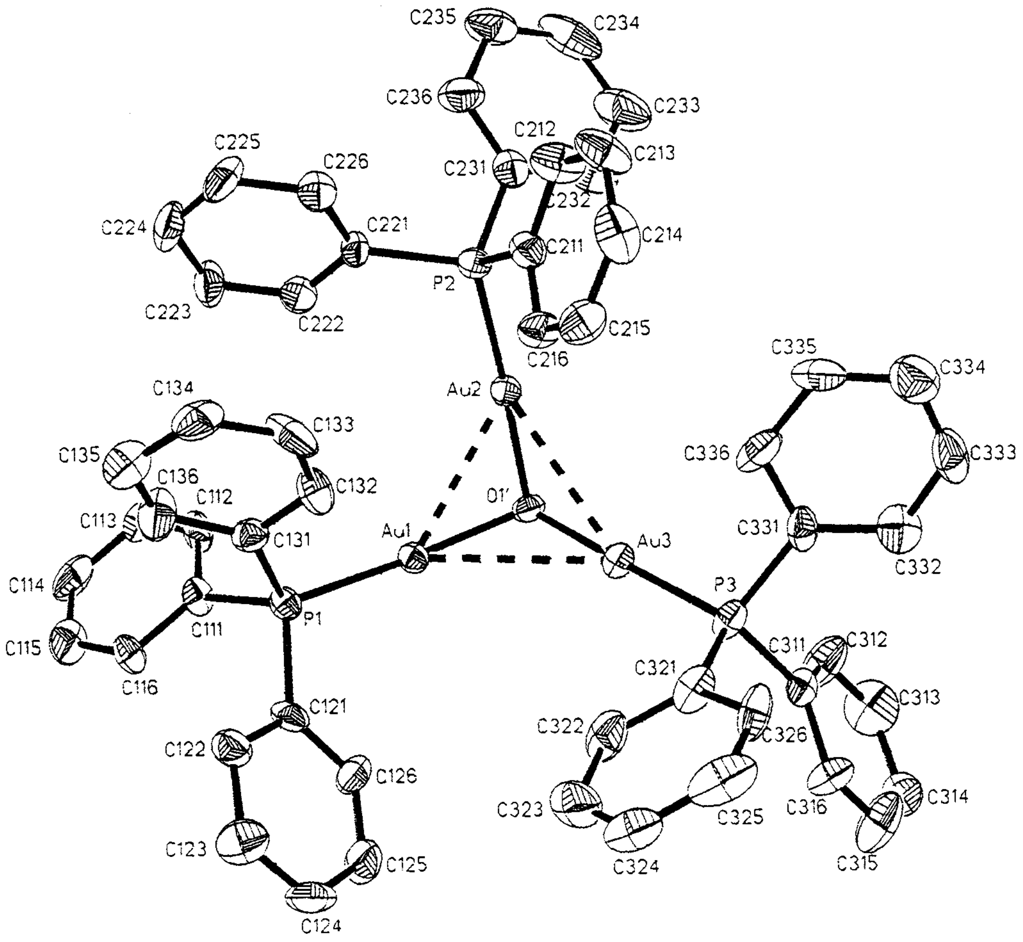

Fig. 2. The structure of the cation and numbering scheme in **2**. The hydrogen atoms are omitted.

linear fragment [20]. Another known aurated 2-hydroxypyridine-(6-methylpyridonato-*N*)-triphenylphosphinegold(I) (investigated as benzene–H_2O solvate) [21] has a monomeric structure in crystal. This compound also exists as an N-derivative with the Au–N bond distance equal to 2.078(9) Å.

Table 4
Selected bond lengths (Å) and bond angles (°) for **2**[a]

Au(1)–Au(2)	2.939(2)	Au(3)–P(3)	2.212(6)
Au(1)–Au(2) # 1	3.162(2)	O(5)–C(4)	1.24(3)
Au(1)–Au(3)	3.171(2)	N(1)–C(2)	1.34(5)
Au(2)–Au(3)	3.114(2)	N(1)–C(6)	1.37(5)
Au(1)–O(1′)	2.04(1)	C(2)–C(3)	1.36(5)
Au(1)–P(1)	2.226(5)	C(3)–C(4)	1.43(4)
Au(2)–O(1′)	2.08(1)	C(4)–C(5)	1.39(4)
Au(2)–P(2)	2.220(5)	C(5)–C(6)	1.39(4)
Au(3)–O(1′)	1.98(1)		
O(1′)–Au(1)–P(1)	173.3(4)	C(3)–C(2)–N(1)	122(3)
O(1′)–Au(2)–P(2)	176.3(4)	C(2)–C(3)–C(4)	125(3)
O(1′)–Au(3)–P(3)	177.4(4)	O(5)–C(4)–C(5)	126(3)
Au(1)–O(1′)–Au(2)	90.8(5)	O(5)–C(4)–C(3)	123(3)
Au(1)–O(1′)–Au(3)	104.0(6)	C(5)–C(4)–C(3)	110(3)
Au(2)–O(1′)–Au(3)	100.3(5)	C(6)–C(5)–C(4)	125(3)
C(2)–N(1)–C(6)	118(3)	C(5)–C(6)–N(1)	120(3)

[a] Symmetry transformations used to generate equivalent atoms: # 1 −*x*, −*y*, −*z*.

The geometry of the monomers in **1** is somewhat different. In one fragment (at Au(2)), the Au(2)···O(5′) intramolecular distance, 2.97(1) Å, is rather short and corresponds to a secondary bond. The pattern of angular distortion at the N(1′) and C(2′) atoms confirms the existence of this weak interaction. Actually, C(6′)N(1′)Au(2) and C(3′)C(2′)O(5′) (125.8(7) and 126(1)°) angles, outer with respect to the chelate cycle, are increased compared to the corresponding inner C(2′)N(1′)Au(2) and N(1′)C(2′)O(5′) angles (111.9(7) and 121.1(9)°), which reflects the tendency of the gold and oxygen atoms to move closer together. Such a tendency although less pronounced is also observed for the above-mentioned 6-methylpyridonato-*N*-triphenylphosphinegold(I) where the Au···O intramolecular distance is somewhat longer (3.026 Å) [21]. In the second dinitropyridone fragment of **1** (at Au(1)), the Au···O distance is longer, 3.11(1) Å, and the similar distortion of the bond angles at N(1) is very small (119.6(7) and 118.7(6)°), although this distortion is rather significant at C(2) (128.2(9) and 118.6(8)°). In the dimer, the O(5)

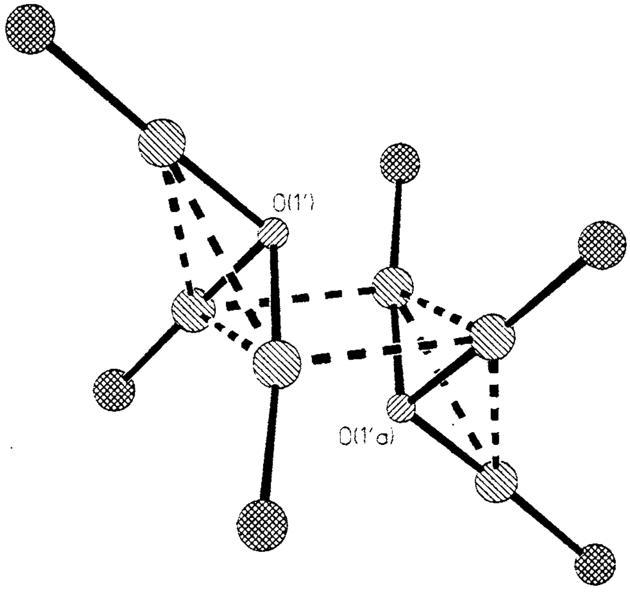

Fig. 3. The schematic diagram of a dimeric cation in **2**. All Ph rings are omitted for simplicity.

atom is situated above the Au···Au line and equally spaced from both gold atoms (the second Au···O distance is 3.14(1) Å). A geometrical calculation shows that one lone pair of oxygen is directed to the region between the gold atoms. Such a geometry agrees well with the idea that a weak interaction exists between the O(5) atom and both Au atoms in this system.

Because both gold atoms are bonded to the nitrogen atoms, the geometrical parameters of the heterocycles exhibit a tendency for the quinoid pattern of the bond-length distribution, with the multiple bonds located between the C(3)–C(4) (C(3′)–C(4′)), C(5)–C(6) (C(5′)–C(6′)), and C(2)–O(5) (C(2′)–O(5′)) atoms.

2.5. X-ray structure of **2**

Product **2** represents a salt of deprotonated 4-hydroxy-3,5-pyridine with tris(triphenylphosphine gold)oxonium (Fig. 2). Selected bond lengths and bond angles in **2** are given in Table 4.

The triaurated oxonium cation has a non-planar structure. The Au–O and Au–P bond lengths vary within 1.98(1)–2.08(1) Å and 2.212(6)–2.226(5) Å, respectively. These values are typical for compounds containing a linear O–Au–P fragment [20]. The bond angles at the central oxygen atom ranges from 90.8(5)° to 104.0(5)°. Even the largest value is smaller than the tetrahedral one. A similar peculiarity was observed for other triaurated oxonium cations in the structure with the BF_4^- anion [22] and in the structure with CH_2Cl_2 solvate [23]. Such a reduction in angles is explained by aurophilic interactions. The Au···Au distances 2.939(2)–3.171(2) Å also lie in the above-mentioned range, typical for this interaction.

The structural data for mercurated oxonium show that the cation has almost planar geometry as distinct from similar gold compounds. In the structures containing $HO(Hg)_2^+$ [24–26], the Hg–O–Hg angle vary within 119.8–126.2° and, in the structure containing $O(Hg)_3^+$ [27], the angles at oxygen are 112.6, 118.8, and 118.8°. This difference may be associated with the fact that mercury does not form a metal···metal secondary bond, which confirms our suggestion of the determining structural role of aurophilic interactions in these structures.

In crystal, two cations are combined in a centrosymmetric dimer through two Au···Au interactions. The diagram of this dimer is shown in Fig. 3.

It is important that, according to all experimental data, triaurated oxonium has a dimeric structure in crystal in spite of the fact that different counterions or solvate molecules determine different packing conditions. In such a dimer, the Au···Au distances between Au atoms belonging to different monomers are comparable with those between Au atoms of the same monomer; in **2**, both Au–Au distances between monomers are equal to 3.162(2) Å. Based on this observation, we may conclude that triaurated oxonium will form a hexanuclear Au···Au bonded dimer regardless of its chemical environment.

The reason why salt rather than the neutral *N*- or *O*-substituted gold compound forms in the second reaction is not quite clear. We suggest that a weak Au···O interaction plays a definite role in the stabilization of neutral product **1**. Such a supporting effect is impossible in the case of the second reaction because the nitrogen and oxygen atoms are too distant from each other in the ligand.

In the crystal of **2**, two anions form a centrosymmetric dimer stabilized by weak hydrogen bonds with two water molecules (Fig. 4).

In spite of the fact that the O···O and O···N distances (3.00(5) and 2.94(5) Å, respectively) are rather long, the mutual arrangement of the two anions and two water molecules corresponds to a H-bonded associate. The geometrical parameters of the anion are close to those observed in tetrafluoro-4-pyridinolate and tetrachloro-4-pyridinolate salts with diethylammonium [28] and 1-benzyl-1,1-dimethylhydrazinium [29].

3. Conclusions

This report presents our attempt to understand the role of weak interactions of different types in the formation and stabilization of some specific structures of Au(I) compounds. We show that potentially tautomeric organic compounds of similar structure may undergo an auration reaction to give unpredictable, structurally different products. We compared Au(I) compounds

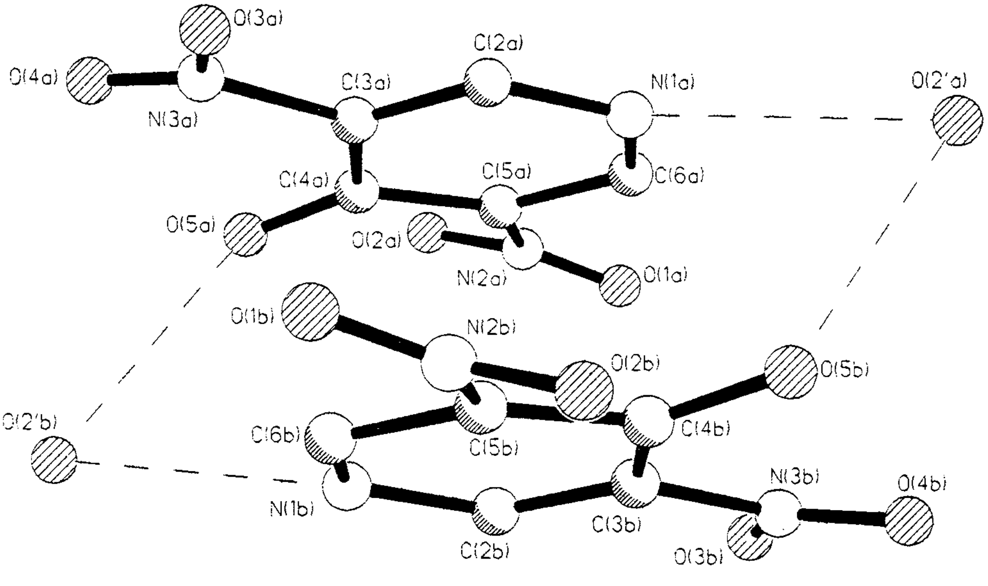

Fig. 4. The structure of the hydrogen-bonded centrosymmetric associate of the two anions and two water molecules in **2**.

with the structurally related Hg(II) and organic compounds. Even this cursory comparison reveals very peculiar chemical and structural properties of Au(I) compounds distinguishing them from related organic and organomercury(II) compounds.

4. Experimental

4.1. Synthesis of 1-(triphenylphosphinegold)-3,5-dinitropyridone-2(1H)

3,5-Dinitro-2-hydroxypyridine ($T_{\text{melt}} = 175°\text{C}$) was synthesized according to the standard method [30].

To 0.15 g (0.91 mmol) of 2-hydroxy-3,5-dinitropyridine in 30 ml of dehydrated THF, 0.1 g of potash, 0.5 ml of distilled water, and 0.4 g (0.27 mmol) of tris(triphenylphosphinegold)oxonium tetrafluorobarate were added. The reaction mixture was agitated until complete dissolution of the oxonium salt (for 10 min). Then, the solution was dried with potash, filtered off, and the solvent was evaporated in vacuum. 1-(Triphenylphosphinegold)-3,5-dinitropyridone-2(1*H*) was obtained in quantitative yield as light yellow powder-like substance, decomposition above 180°C.

For $C_{27}H_{25}AuN_3O_6P$, calc. for solvate with 1 THF (%): C, 45,32; H, 3.52, N, 5.87. Found, C, 45,31; H, 3.32; N, 6.07.

The crystals suitable for X-ray diffraction study were grown from the THF–cyclohexane mixture.

4.2. Synthesis of tris(triphenylphosphinegold)oxonium 3,5-dinitro-4-pyridinolate

3,5-Dinitro-4-hydroxypyridine ($T_{\text{melt}} = 175°\text{C}$) was synthesized according to the standard method [31].

Table 5
IR spectrum of **1** and initial 3,5-dinitro-2-hydroxypyridine in the ranges of ν(OH), ν(NH), ν(C=O), ν(C≡C), and $\nu(NO_2)$ (cm^{-1})

Relation	Solvent	**1**	Initial pyridine
ν(OH), ν(NH)	Nujol		3220 m
ν(C=O)	Nujol	1644 s	1700 s, 1690 s
	CH_3CN	1660 s	1718 s, 1703 s
	THF	1663 s	1717 s, 1705 s
ν(C=C)	Nujol	1590 w	1618 m
	CH_3CN	1594 w	1625 m
	THF	1593 w	1624 m
$\nu_{as}(NO_2)$	Nujol	1550 s	1570 s
	CH_3CN	1555 s	1575 s
	THF	1552 s	1579 s
$\nu_s(NO_2)$	Nujol	1319 s, 1280 m	1330 s, 1250 s

Table 6
IR spectrum of **2** and initial 3,5-dinitro-4-hydroxypyridine in the ranges of ν(OH), ν(NH), ν(C=O), ν(C=C), and $\nu(NO_2)$ (cm^{-1})

Relation	Solvent	**2**	Initial pyridine
ν(OH), ν(NH)	Nujol		3510
	THF		3525 s, 3440 m, 3250 m
ν(C=O)	Nujol	1633 s, 1610 m	1663 s, 1630 w
	THF	1645 s, 1614 w	1685 s, 1640 w
ν(C=C)	Nujol	1553 w	1600 m
	THF		1640 m
$\nu_{as}(NO_2)$	Nujol	1504 m	1500 m
$\nu_s(NO_2)$	Nujol	1347 m, 1266 s	1350 s, 1280 m

Table 7
Crystal data, data collection, structure solution and refinement parameters for **1** and **2**

	1	**2**
Empirical formula	$C_{51}H_{44}Au_2N_6O_{10.5}P_2$	$C_{59}H_{48}Au_3N_3O_6P_3 \cdot H_2O$
Formula weight	1406.9	1596.82
Color, habit	Yellow, plate	Colorless, block
Crystal size (mm)	0.08 × 0.12 × 0.36	0.20 × 0.12 × 0.16
Crystal system	Monoclinic	Triclinic
Space group	$P2_1/n$	$P\bar{1}$
Unit cell dimensions		
a (Å)	16.772(2)	13.844(6)
b (Å)	14.659(8)	13.913(6)
c (Å)	20.700(3)	14.723(7)
α (°)	90	77.49(4)
β (°)	90.425(9)	83.84(4)
γ (°)	90	87.80(4)
Volume (Å^3)	5089(3)	2752(2)
Z	4	2
Density (calculated) (g cm^{-3})	1.836	1.924
Absorption coefficient (mm^{-1})	5.884	8.119
F(000)	2760	1522
Diffractometer	Enraf-Nonius CAD4	Enraf-Nonius CAD4
Temperature (K)	293	293
Radiation (λ, Å)	Mo–K$_\alpha$ (0.71073)	Mo–K$_\alpha$ (0.71073)
Scan mode	$\omega/2\theta$	$\omega/2\theta$
Scan width (°)	$0.9 + 0.35\tan(\theta)$	$0.8 + 0.35\tan(\theta)$
Min/max scan rate (° min^{-1})	2/8	2/8
Theta range (°)	2.09–27.89	2.09–26.80
Index ranges	$-22 \leq h \leq 20$ $0 \leq k \leq 18$ $0 \leq l \leq 25$	$-17 \leq h \leq 17$ $-16 \leq k \leq 15$ $-17 \leq l \leq 0$
Reflections collected	8472	5539
Independent reflections	8259 [R(int) = 0.0367]	5539 [R(int) = 0.0000]
Absorption correction	Empirical (psi scan)	DIFABS
Max. and min. transmission	0.9543 and 0.6718	1.135 and 0.885
Decay correction	None	None
Data/restraints/parameters	8231/5/628	5503/0/677
Goodness-of-fit on F^2	0.989	1.006
Final R indices [$I > 2\sigma(I)$]	$R_1 = 0.0378$, $wR_2 = 0.0945$	$R_1 = 0$ .0543, $wR_2 = 0.1566$
R indices (all data)	$R_1 = 0.1094$, $wR_2 = 0.1270$	$R_1 = 0.0585$, $wR_2 = 0.1739$
Extinction coefficient	0.00000(7)	0.0000(2)
Largest difference peak and hole (e A^{-3})	2.034 and −1.083	2.137 and −1.941

To 20 ml of anhydrous THF, 0.08 g (0.405 mmol) of 4-hydroxy-3,5-dinitropyridine, 0.2 g of potash, 0.5 ml of distilled water were added. In 5 min, the orange precipitate of the initial compound dissolved, and raspberry potassium 3,5-dinitro-4-pyridinolate precipitated. In 10 min, 2ml of ethanol and 0.2 g (0.135 mmol) of tris(triphenylphosphinegold)oxonium tetrafluorobarate were added. After agitating for 30 min, the raspberry precipitate dissolved. The solution was dried with potash, filtered of and the solvent was evaporated in vacuum. Tris(triphenylphosphinegold)oxonium 3,5-dinitro-4-pyridinolate was obtained in quantitative yield in the form of yellow powder-like substance, decomposition above 170°C.

For $C_{59}H_{47}Au_3N_3O_6P_3$, calc. (%): C, 44,91; H, 2.98, N, 2.66; Found, C, 44,82; H, 3.02; N, 2.75.

The crystals suitable for X-ray diffraction study were grown from the THF–petroleum ether mixture.

4.3. IR and UV spectroscopy

IR spectra were recorded on a Specord M-82 instrument in the cells of CaF_2 ($d = 0.01$–0.06 cm). UV spectra were measured on a Specord M-40 instrument in quartz cells ($d = 0.1$ cm). Concentrations of the compounds to be investigated in acetonitrile and THF were 0.005–0.02 M. IR spectra of **1** and **2** and the corresponding initial organic compounds are given in Tables 5 and 6, respectively.

4.4. Quantum chemical calculations

The calculations were performed using the SCF and MP2 methods with the 3-21G and 6-31G** basis sets. Full geometry optimization was performed for all the structures under consideration. The GAMESS [32] and GAUSSIAN [33] program packages were used in these calculations.

4.5. X-ray crystallography of **1** and **2**

Details of the X-ray experiment are given in Table 7. The experimental data were collected on an ENRAF Nonius CAD4 diffractometer using graphite monochomatized Mo–K_α radiation. Experimental reflections were corrected for Lorents and polarization.

The hydrogen atoms were calculated geometrically (d(C–H) = 0.94 Å) and included in the refinement using the riding model with B_{iso} equal to $1.5B_{eq}$ of the parent carbon atom. The structures were refined in the anisotropic approximation for the non-hydrogen atoms.

In the structure of **1**, two solvent molecules—THF and cyclohexane—were found during the structure solution. The cyclohexane molecule is situated around a symmetry center. The THF molecule is disordered and is, probably, characterized by not full occupation: The l.s. refinement gives the site occupation factor for the molecule equal to 0.5. We failed to distinguish between the oxygen and carbon atom positions.

In the structure of **2**, an additional rather high peak of electron density was found in the difference Fourier synthesis. This peak was considered as a water oxygen. The refinement of this atom gave its position which satisfy a representation about the above-mentioned hydrogen-bonded associate.

Both structures were solved and refined using the SHELXS-86 [34] and SHELXL-93 [35] software.

Complete lists of bond lengths and angles, atomic coordinate are deposited at the Cambridge Crystallographic Data Center.

Acknowledgements

We thank the Russian Foundation for Basic Research (Grants 98-03-33142a and 96-03-33906a) and the Royal Society for financial support of this work.

References

[1] L.G. Kuz'mina, N.V. Dvortsova, E.I. Smyslova, K.I. Grandberg, Russ. J. Inorg. Chem. 7 (1992) 1420.

[2] L.G. Kuz'mina, J. Inorg. Chem. 38 (1993) 918.

[3] L.M. Epshtain, L.D. Ashkinadze, L.S. Golovchenko, V.M. Pochevskayua, D.N. Kravtsov, Izv. AN SSSR, Ser. Khim., 1978, 1030.

[4] V.P. D'yachenko, Vestnik of Moscow State University, Chem. 3 (1976) 358.

[5] L.M. Epshtain, L.M. Saitkulova, E.S. Shubina, L.S. Golovchenko, D.N. Kravtsov, Russ. Chem. Bull. 45 (1996) 1749.

[6] A. Kvick, Acta Crystallogr. B32 (1976) 220.

[7] A. Kvick, I. Olovsson, Ark. Kimi. 30 (1969) 71.

[8] U. Ohms, H. Guth, E. Hellner, H. Dannohl, A. Schweig, Z. Cristallogr. 169 (1984) 185.

[9] V. Cody, A. Wojtezak, Acta Crystallorg. C47 (1991) 787.

[10] J. Almlof, A. Kvick, I. Olovsson, Acta Crystallogr. B27 (1971) 1201.

[11] S. Shiotani, H. Morita, M. Inoue, T. Ishida, Y. Iitaka, A. Itai, J. Heterocycl. Chem. 21 (1984) 725.

[12] Y. Nakatsuji, J.S. Bradshaw, Pui-Kwan Tse, G. Arena, B.E. Wilson, N.K. Dalley, R.M. Izatt, J. Chem. Soc., Chem. Commun. (1985) 749.

[13] J.S. Bradshaw, M.L. Colter, Y. Nakatsuji, N.O. Spencer, M.F. Brown, R.M. Izatt, G. Arena, P.-K. Tse, B.E. Wilson, J.D. Lamb, N.K. Dalley, F.G. Morin, D.M. Grant, J. Org. Chem. 50 (1985) 4865.

[14] J.S. Bradshaw, Y. Nakatsuji, P. Huszthy, B.E. Wilson, N.K. Dalley, R.M. Izatt, J. Heterocycl. Chem. 23 (1986) 353.

[15] L.M. Toledo, J.W. Lauher, F.W. Fowler, Chem. Mater. 6 (1994) 1222.

[16] L.G. Kuz'mina, T.V. Baukova, A.V. Churakov, V.S. Kuz'min, N.V. Dvortsova, Soviet J. Coord. Chem. 23 (1997) 279.

[17] J.P. Fackler Jr., R.J. Staples, A. Elduque, T. Grant, Acta Crystallogr. C50 (1994) 520.

[18] L.G. Kuz'min, O.Yu. Burtseva, N.V. Dvortsova, M.A. Porai-Koshits, E.I. Smyslova, Sov. J. Coord. Chem. 15 (1989) 466.

[19] P. Pyykkö, Li Jian, N. Runeberg, Chem. Phys. Lett. 218 (1994) 133.

[20] L.G. Kuz'mina, Metalloorgan. Khim. 5 (1992) 744.

[21] F. Bonati, A. Burini, B.R. Pietrony, B. Bovio, J. Organomet. Chem. 296 (1985) 301.

[22] A.N. Nesmeyanov, E.G. Perevalova, Yu. T. Struchkov, M.Yu. Antipin, K.I. Grandberg, V.P. Dyadchenko, J. Organomet. Chem. 201 (1980) 343.

[23] Yi Yang, V. Ramamoorthy, P.R. Sharp, Inorg. Chem. 32 (1993) 1946.

[24] B.K. Nicholson, A.J. Whitton, J. Organomet. Chem. 306 (1986) 139.

[25] D. Grdenic, D. Matkovic-Calogovic, M. Sikirika, J. Organomet. Chem. 319 (1987) 1.

[26] Zhiping Zheng, C.B. Knobler, C.E. Curtis, M.F. Hawthorne, Inorg. Chem. 34 (1995) 432.

[27] D. Grdenic, M. Sikirika, D. Matkovic-Calogovic, A. Nagl, J. Organomet. Chem. 253 (1983) 283.

[28] R.G. Pritchard, A.J. Adamson, R.E. Banks, W. Jondi, A.E. Tipping, Acta Crystallogr. C47 (1991) 1124.

[29] L. Julia, H. Suschitzky, J.C. Barnes, C.D.S. Tomlin, J. Chem. Soc., Perkin Trans. 1 (1983) 2507.

[30] T. Takanashi, F. Yoneda, Chem. Pharm. Bull. (Tokyo) 6 (1958) 442 (C.A. 53 (1959) 22296).

[31] M. Fujimoto, Pharm. Bull. (Japan) 4 (1956) 77 (C.A. 51 (1957) 5069g).

[32] M.W. Schmidt, K.K. Baldridge, J.A. Boatz, S.T. Elbert, M.S. Gordon, J.H. Jensen, S. Koseki, N. Matsunaga, K.A. Nguyen, S.J. Su, T.L. Winddus, M. Dupuis, J.A. Montgomery, J. Comput. Chem. 14 (1993) 1347.

[33] M.J. Frisch, G.W. Trucks, H.B. Schlegel, P.M.W. Gill, B.G. Johnson, M.A. Robb, J.R. Cheeseman, T. Keith, G.A. Petersson, J.A. Montgomery, K. Raghavachari, M.A. Al-Laham, V.G. Zakrzewski, J.V. Ortiz, J.B. Foresman, J. Cioslowski, B.B. Stefanov, A. Nanayakkara, M. Challacombe, C.Y. Peng, P.Y. Ayala, W. Chen, M.W. Wong, J.L. Andres, E.S. Replogle, R. Gomperts, R.L. Martin, D.J. Fox, J.S. Binkley, D.J. Defrees, J. Baker, J.P. Stewart, M. Head-Gordon, C. Gonzalez, J.A. Pople, Gaussian, Inc., Pittsburgh, PA, 1995.

[34] G.M. Sheldrick, Acta Crystallogr. A46 (1990) 467.

[35] G.M. Sheldrick, SHELXL-93. Program for the Refinement of Crystal Structures, University of Göttingen, 1993, Germany.